Evaluation of optical properties of retroreflectors

for quantum illumination

Genta Masada

Quantum ICT Research Institute, Tamagawa University
6-1-1 Tamagawa-gakuen, Machida, Tokyo 194-8610, Japan

Evaluation of optical properties of retroreflectors for quantum illumination

Genta Masada

Quantum ICT Research Institute, Tamagawa University

6-1-1 Tamagawa-gakuen, Machida, Tokyo 194-8610, Japan

E-mail: g.masada@lab.tamagawa.ac.jp

Abstract—**In quantum illumination, one of the entangled light is emitted toward a target object. When two-mode squeezed light is used as the light source, the reflected light from the target object is detected by homodyne measurement. In order to detect the reflected light with high efficiency, it is expected that the spatial mode of the reflected light is unchanged as well as improving the reflectance at the target object. We are investigating a method to improve the light detection efficiency by attaching a retroreflector to the target object. In this study, we evaluated the reflection characteristics of a retroreflector and observed the intensity distribution and interference of the reflected light.**

I. INTRODUCTION

There is a great deal of interest in highly sensitive sensing technology using quantum entanglement. Quantum illumination is a theory aimed at improving target detection sensitivity [1], [2], [3]. We are considering applying two-mode squeezed light to quantum illumination [4] . In quantum illumination, one entangled light wave is emitted toward a target in an atmospheric disturbance. The light wave reflected by the target is detected by homodyne measurement using optical interference.

The light reflection characteristics of the target object differ depending on the material and surface condition of the object. For example, in materials such as glass and metal, specular reflection occurs as shown in Fig. 1(a). For ideal specular reflection, the reflected light travels in a different direction than the incident light, except when the incident angle is zero degrees. Since the light source and photodetector are co-located in quantum illumination, it is difficult to receive the specularly reflected light at the detector. Diffuse reflection as shown in Fig. 1(a) usually occurs on a rough surface. The diffusely reflected light scatters in various directions, and its intensity per unit area attenuates in inverse proportion to the square of the distance from the target object. Since the power of quantum light sources is usually very weak, attenuation of reflected light is a serious problem. So, the range in which the target object can be detected is limited to a short distance. In order to extend the detection distance, it is important to improve the reflectance on the surface of the target object and improve the light detection efficiency. Furthermore, especially in quantum illumination, since the reflected light from the target object is detected by homodyne measurement, it is also important that the

direction and spatial mode of the reflected light do not change.
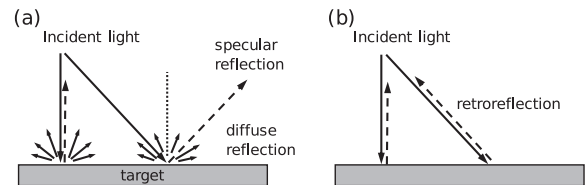
Fig. 1. Classification of light reflection on target surfaces (a) specular reflection and diffuse reflection, (b) retroreflection

In order to solve such problems, we are investigating the use of retroreflection in quantum illumination. Retroreflection is a reflection phenomenon in which incident light from any direction returns to the direction of incidence as shown in Fig. 1(b). A mirror having such a retroreflection function is called a retroreflector. By using a retroreflector, it is expected to be able to efficiently detect reflected light from target objects in a wide range of angles and in various directions. In the application of quantum illumination to improve road traffic safety, we think that the method of attaching high-performance retroreflectors to the bumpers of automobiles and clothing of pedestrians is effective. Such retroreflectors are already widely used in road signs and the like. However, the use of retroreflectors in quantum illumination requires much higher retroreflectance and lower beam divergence performance than conventional ones.

In recent years, high-performance retroreflectors for aerial displays have been developed, improving the retroreflectance and the spread of reflected light. The purpose of this work is to conduct an evaluation experiment of the optical properties of a high-performance retroreflector for aerial displays. The retroreflector was irradiated with a laser beam, and the reflectance and beam spread of the reflected light were evaluated. We also observed the interference of retroreflected light. Then, we examined the technical issues that would arise when retroreflectors are applied to quantum illumination.

II. RETROREFLECTOR

There are various types of Retroreflectors. In this study, we used the RF-A series of retroreflectors developed
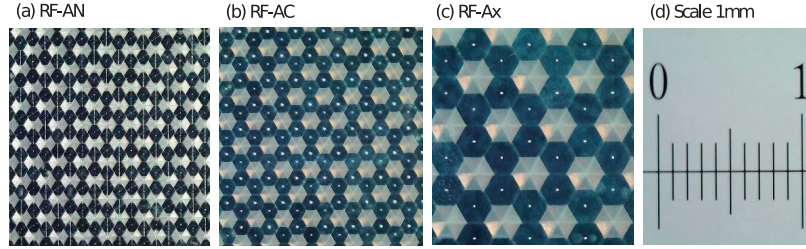
Fig. 2. Observation results of the surface layer of the retroreflector: (a) RF-AN, (b) RF-AC, (c) RF-Ax, (d) scale (1 mm).

for aerial displays by Nippon carbide industries co., inc. [5], [6]. The RF-A series has high retroreflectance and controls the direction and spread of reflected light. These are resin sheets with a thickness of about 1 mm. Fig. 2 shows photographs of the surface layer of the retroreflector observed with a stereoscopic microscope, (a) RF-AN, (b) RF-AC, (c) RF-Ax, and (d) scale (1 mm). As shown in the photographs, inside the retroreflector, triangular pyramid-shaped fine prism elements are arranged without gaps. It can be seen that the size of the prism is about 0.1 mm to 0.4 mm, increasing in order of RF-AN, RF-AC, and RF-Ax. In each prism element, three faces are arranged perpendicular to each other [6]. The dark areas in the photographs are the areas that contribute to retroreflection. Light incident on the surface is sequentially reflected by three surfaces of the prism element and retroreflected in the same direction as the incident direction. Areas that look white are areas that do not contribute to retroreflection. Light incident near the three corners of the triangular pyramid shaped prism element is reflected once or twice and emitted to the outside.

III. EVALUATION OF REFLECTION CHARACTERISTICS BY EXPERIMENTAL LAYOUT 1

In this study, we first measured the retroreflectance of retroreflectors using the experimental layout shown in Fig. 3. A continuous wave Nd:YAG laser (CrystaLaser, CL1064-400-S) with a wavelength of 1064 nm was used as a light source. Although not shown in the figure, the laser beam emitted from the light source is collimated by a spherical lens with a focal length of 500 mm, and the beam diameter is adjusted to about 1.8 mm. Although the polarization of the laser beam is p-polarization (p-pol), it is adjusted to s-polarization (s-pol) by half wave plate HWP for the convenience of later experiments. In order to measure the retroreflectance, it is necessary to measure the incident light intensity and the reflected light intensity and calculate their ratio. Therefore, it is necessary to spatially separate the incident light and the retroreflected light. The incident light first enters the beam splitter BS with a reflectance of 0.5. The reflected laser beam is reflected by retroreflector RR and enters the beam splitter BS again. The transmitted beam through

the beam splitter BS was focused with a lens, and its intensity was measured with power meter PM. Let I_o be the intensity of the output light measured at this time. Similarly, the intensity I_i of input light incident on the beam splitter BS from the light source was also measured, and the retroreflectance R was calculated by I_o/I_i. When measuring the retroreflectance, the retroreflector RR was rotated in the θ direction. The retroreflector RR was also rotated in the ϕ_R direciton which is in a plane perpendicular to the incident optical axis while keeping the angle θ of the retroreflector at 0°.
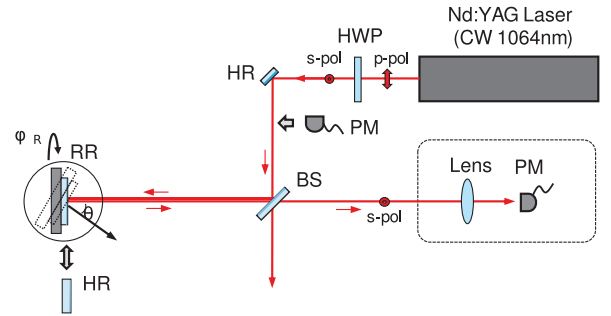
Fig. 3. Experiment layout 1 for evaluation of retroreflection with beam splitter BS

Fig. 4 shows the measurement results of the retroreflectance in the experimental layout 1. Green triangles correspond to RF-AN results, red squares to RF-AC results, and blue circles to RF-Ax results. (a) is the result when the retroreflector RR is rotated in the θ direction to change the angle of the incident beam. The highest value of retroreflectance was higher in the order of RF-Ax, RF-AC, and RF-AN. When the angle θ is 0°, the retroreflectance of RF-Ax exceeds 0.1. Retroreflection was confirmed at a wide range of angles θ in all retroreflectors. The full width of the angle θ at which the retroreflectance is halved was approximately 80° in each case.

For comparison, the reflectance was 0.25 when the high reflectance mirror HR was used instead of the retroreflector. This is a result of the incident beam passing through the beam splitter BS twice, thus reducing its intensity by a factor of four. However, the reflected light returns in the direction of the incident light only when

(a)

(b)
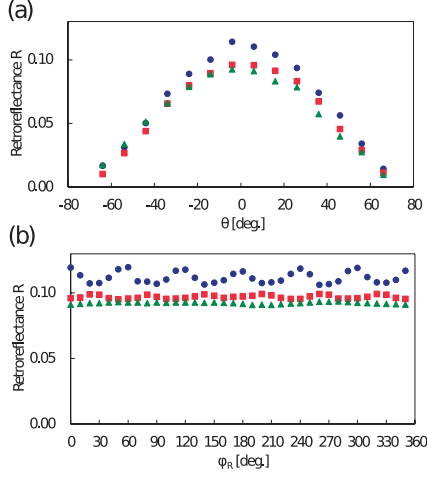
Fig. 4. Measurement result of retroreflectance. Green triangles correspond to RF-AN, red squares to RF-AC, and blue circles to RF-Ax results. (a) rotate the retroreflector in the θ direction, (b) rotate the retroreflector in the ϕ_R direction with the angle θ set to 0°.

the incident angle θ is 0°. Even a slight deviation of the incident angle θ from 0° immediately caused the reflected light to deviate from the power meter PM, making it impossible to measure its intensity.

(b) is the retroreflectance when the retroreflector is rotated in the ϕ_R direction while keeping the angle θ at 0°. There was little change in retroreflectance between RF-AN and RF-AC. However, in the RF-Ax, the retroreflectance varied periodically during one rotation of the retroreflector, repeating an increase and a decrease six times. This is because the retroreflector is composed of triangular prisms, and as shown in Fig. 2, it reflects the six-fold symmetrical structure.

IV. EVALUATION OF REFLECTION CHARACTERISTICS BY EXPERIMENTAL LAYOUT 2

In the experimental layout 1 of Fig. 3, the laser beam passes through the beam splitter BS twice, so the output light intensity I_o is reduced by a factor of four. As a result, the reflectance from the retroreflector is apparently lowered. To overcome such problems, we used a polarization beam splitter PBS and a quarter wave plate QWP instead of the beam splitter [7], as shown in experimental layout 2 in Fig. 5. The incident beam with s-polarization (s-pol) is totally reflected by the polarization beam splitter PBS. The laser beam that has passed through quarter wave plate QWP becomes circular polarizaiton. The beam reflected by the retroreflector passes through the quarter wave plate QWP again, becomes p-polarization (p-pol), and passes through the polarization beam splitter PBS. Such an optical system is expected to improve the reflectance R by a factor of 4 compared to the experimental layout 1 shown in Fig. 3.

In experimental layout 2 shown in Fig. 5, we not only measured the retroreflectance, but also observed

the intensity distribution of the laser beam with a beam profiler (Ophir, BM-USB-SP928-OSI). The beam profiler was placed 20 cm away from the retroreflector. For comparison, the intensity distribution was also measured when high reflection mirror HR was installed instead of retroreflectors.
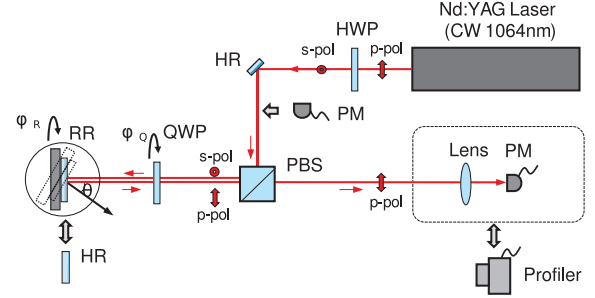
Fig. 5. Experimental layout 2 for evaluation of retroreflection with polarization beam splitter PBS

(a)

(b)

(c)
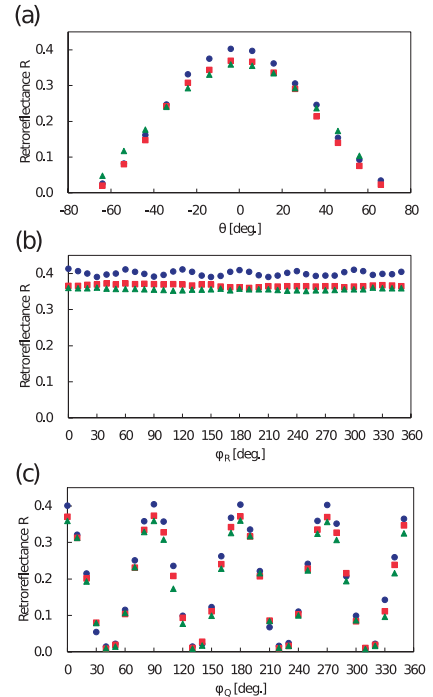
Fig. 6. Measurement result of retroreflectance. Green triangles correspond to RF-AN, red squares to RF-AC, and blue circles to RF-Ax results. (a) rotate the retroreflector in the θ direction, (b) rotate the retroreflector in ϕ_R direction when the retroreflector angle θ is 0°, (c) rotate the quater wave plate in ϕ_Q direciton when the retroreflector angle θ is 0° and ϕ_R is 0°.

Fig. 6 shows the measured retroreflectance in experimental layout 2 using polarization beam splitter PBS. Similar to Fig. 4, green triangles indicate RF-AN results, red squares indicate RF-AC results, and blue circles indicate RF-Ax results. (a) is the result when the retroreflector
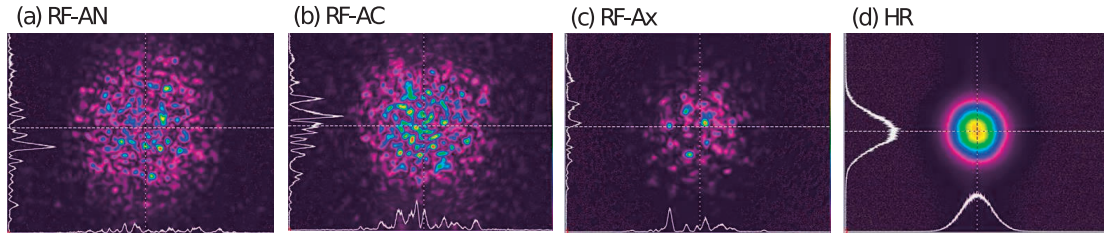
Fig. 7. Observation results of the intensity distribution of the reflected beam in experimental layout 2. (a) RF-AN, (b) RF-AC, (c) RF-Ax are used as retroreflection mirrors, and (d) total reflection mirror HR is used instead of retroreflection mirrors. The active area size of the image sensor of the beam profiler is 5.3 mm x 7.1 mm.

is rotated in the θ direction. (b) is the result when the retroreflector is rotated in the ϕ_R direction while keeping the angle θ at $0°$. The dependence on each angle is the same as in Fig. 4. It is clear that the retroreflectance is improved by about four times compared to the results of Fig. 4. Especially for RF-Ax, the retroreflectance exceeded 0.4 when the angle θ was $0°$. This is a benefit of using polarization beam splitter PBS and quarter wave plate QWP. For comparison, the reflectance was almost 1 when the retroreflector was replaced with a high reflectance mirror HR in the same experimental layout.

(c) shows the retroreflectance when the angle ϕ_Q of the quarter-wave plate QWP is changed while the angles θ and ϕ_R are zero degrees. During one rotation of the quarter wave plate QWP, the retroreflectance varied between the maximum value and 0 four times. This is because the polarization direction of the incident beam and the slow axis and fast axis of the quarter wave plate QWP became parallel four times. It is considered that total passage by horizontal polarized light and total reflection by vertical polarized light are repeated four times in the polarization beam splitter PBS. This result indicates that it is necessary to carefully adjust the rotation angle ϕ_Q of the quarter wave plate QWP when improving the retroreflectance with a polarization beam splitter.

Fig. 7 shows the intensity distribution of the laser beam reflected by the retroreflectors, (a) RF-AN, (b) RF-AC, and (c) RF-Ax. (d) is a case where a high reflection mirror HR is used instead of the retroreflector. When using the highly reflective mirror HR, the laser beam remains collimated. On the other hand, it can be seen that the intensity distribution of the retroreflected beam from the retroreflectors spread in the order of RF-Ax, RF-AC, and RF-AN. It can also be seen that noise is superimposed.

V. Observation of optical interference

Next, interference was observed using retroreflected light having the intensity distribution shown in Fig. 7. Fig. 8 shows an optical interferometer including retrore-flectors. The adjustment of the polarization direction is the same as experimental layout 2 in Fig. 5. One of the signal beams split by the beam splitter BS_1 is reflected by
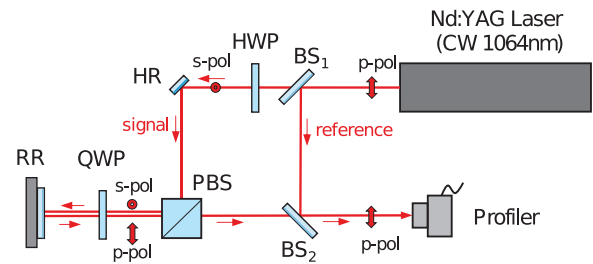
Fig. 8. Experimental layout of an optical interferometer using a retroreflector

the retroreflector RR and then degrades to the intensity distribution shown in Fig. 7(a)-(c). The other reference light is a collimated beam as shown in Fig. 7(d). Although not shown in the figure, the optical path length of the reference light is adjusted by multiple mirrors so that both optical path lengths are equal. Both beams were combined by beam splitter BS_2 and observed by beam profiler.

Fig. 9 shows the results of observing the interference between the signal beam and the reference beam using retroreflectors (a) RF-AN, (b) RF-AC, and (c)RF-Ax, respectively. Although it is not clear enough to measure the visibility, it can be seen that there is a slight fringe pattern due to interference. The intensity distribution of the retroreflected beam is broadened as shown in Fig. 7, and noise is generated, but it can be seen that a small amount of interference remains.

VI. Summary and future prospects

In this study, we measured the reflectance of laser beam and observed the intensity distribution and interference of the reflected beam using retroreflectors developed for aerial displays by Nippon carbide industries co., inc. The angle of retroreflection was in a range of about 80 degrees at full width at half maximum. In addition, in experimental layout 2, in which the polarization of the laser beam was adjusted, a high retroreflectance of 0.4 was observed. Because retroreflectors have high retrore-flectivity, they may become important optical elements for
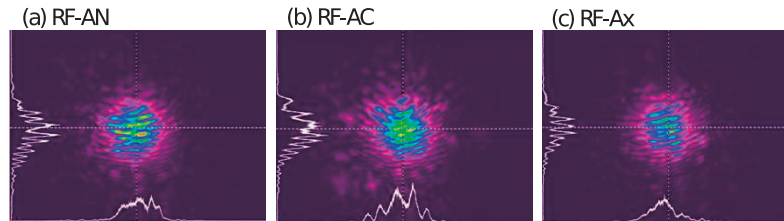
Fig. 9.   Observation results of optical interference when using (a) RF-AN, (b) RF-AC, and (c) RF-Ax as retroreflectors.

quantum illumination using low-power quantum light. On the other hand, it was found that the intensity distribution of the retroreflected beam was broadened and noise was generated. Also, the residual interference was very low. When applying retroreflectors to quantum illumination, it is desirable that the spatial mode and interference of the reflected beam remain unchanged. Improvements to the retroreflector are expected in the future. Alternatively, it is necessary to consider improvement methods at the system level, such as introducing an adaptive optics device.

REFERENCES

[1] S. Lloyd, "Enhanced sensitivity of photodetection via quantum illumination," Science **321** 1463-1465, (2008).

[2] S. H. Tan, B. I. Erkmen, V.Giovannetti, S. Guha, S. Lloyd, L. Maccone, S. Pirandola, and J. H. Shapiro,"Quantum illumination with Gaussian states," Phys. Rev. Lett. **101** 253601, (2008).

[3] J. H. Shapiro, and S. Lloyd, "Quantum illumination versus coherent-state target detection," New J. of Phys. **11** 063045, (2009).

[4] G. Masada, "Verification of quantum entanglement of two-mode squeezed light source towards quantum radar and imaging ," Proc. SPIE **10409** Quantum Communications and Quantum Imaging XV, 104090P, (2017).

[5] Nippon carbide industries co., Inc., Aerial Display Reflector RF-A Series, https://www.carbide.co.jp/en/product/rf-a-siries/

[6] "Recent Developments and Prospective Applications of Aerial Display", Edited by Hirotsugu Yamamoto, CMC publishing Co., Ltd. (2018)

[7] N. Kawaguchi, K. Onuki, and H. Yamamoto, "Comparison of divergence angle of retro-reflectors and sharpness with aerial imaging by retro-reflection (AIRR)", IEICE Trans. Elec., vol.**E100-C**, No.11, 958-964, Nov. (2017).